A Space–Time Multiscale Analysis System: A Sequential Variational Analysis Approach

Y. XIE, S. KOCH, AND J. MCGINLEY

NOAA/Earth System Research Laboratory, Boulder, Colorado

S. ALBERS

NOAA/Earth System Research Laboratory, Boulder, and Cooperative Institutes for Research in the Atmosphere, Colorado State University, Fort Collins, Colorado

P. E. BIERINGER

National Center for Atmospheric Research, Boulder, Colorado

M. WOLFSON AND M. CHAN

Lincoln Laboratory, Massachusetts Institute of Technology, Cambridge, Massachusetts

(Manuscript received 6 January 2010, in final form 23 November 2010)

ABSTRACT

As new observation systems are developed and deployed, new and presumably more precise information is becoming available for weather forecasting and climate monitoring. To take advantage of these new observations, it is desirable to have schemes to accurately retrieve the information before statistical analyses are performed so that statistical computation can be more effectively used where it is needed most. The authors propose a sequential variational approach that possesses advantages of both a standard statistical analysis [such as with a three-dimensional variational data assimilation (3DVAR) or Kalman filter] and a traditional objective analysis (such as the Barnes analysis). The sequential variational analysis is multiscale, inhomogeneous, anisotropic, and temporally consistent, as shown by an idealized test case and observational datasets in this study. The real data cases include applications in two-dimensional and three-dimensional space and time for storm outflow boundary detection (surface application) and hurricane data assimilation (three-dimensional space application). Implemented using a multigrid technique, this sequential variational approach is a very efficient data assimilation method.

1. Introduction

It is common in atmospheric data assimilation to treat the observations and model backgrounds as random vectors and to use a statistical approach to maximize the probability for a good analysis (Lorenc 1986). The quality of this analysis depends on the accuracy of the model background and observation error covariance in the hope that the model and observation statistics can provide accurate correlation information between analysis grid points and model states. However, a model background error covariance requires more information than the model error itself. Consider each model background error as a vector of N elements encompassing several state variables and their grid values over all grid points, where N is usually about 10^6 for atmospheric data assimilation. Since the covariance matrix is symmetric, it contains $N \times N/2$ elements. A common statistical practice cannot afford more than ~100 model backgrounds or ensemble members to accumulate the needed covariance. Therefore, there is a tremendous amount of information missing from the computed covariance. Accurate estimation of model background error covariance remains a difficult and challenging problem in atmospheric data assimilation (Bouttier and Courtier 1999). In addition, the derived error covariance from this statistical information is typically singular and thus, some localization or convolution techniques must be used to make the estimated

Corresponding author address: Yuanfu Xie, NOAA/ESRL, R/GSD7, 325 Broadway, Boulder, CO 80305–3328.
E-mail: yuanfu.xie@noaa.gov

DOI: 10.1175/2010MWR3338.1

covariance matrix positive definite. Such localization techniques introduce additional uncertainty into maintaining the limited information in the covariance matrix.

With the deployment of increasingly high-density, accurate, and advanced operational observation systems, more information is now available in the observations than ever before. We can take advantage of this information for atmospheric data assimilation to retrieve the resolvable information before applying a statistical analysis. A standard single variational approach such as three- or four-dimensional variational data assimilation (3DVAR or 4DVAR) (Lorenc 1981; Lewis and Derber 1985; Courtier and Talagrand 1987) may not be adequate, since the required covariance is difficult to obtain at all scales given the flow, location, and time dependency of the covariance. On the other hand, a traditional objective analysis, such as a successive correction approach or Barnes scheme (Koch et al. 1983; Hiemstra et al. 2006), can retrieve resolvable information from conventional observations without requiring any statistical computation. We refer to the method of retrievals that do not require statistical computation as a deterministic approach, and it differs from those methods based on a statistical theory, such as a standard 3DVAR or 4DVAR or ensemble Kalman filter (EnKF). However, a traditional objective analysis approach cannot fully take advantage of the modern observations or utilize physical balance constraints in its analysis, even though such schemes are very effective in handling conventional observations. In summary, the modern data assimilation techniques 3DVAR, 4DVAR, and EnKF, are limited by a lack of sufficient statistical information for a flow-, location-, and time-dependent error covariance matrix, even though they could fully take advantage of modern observation datasets and dynamic balances. On the other hand, a traditional objective analysis can retrieve resolvable information from conventional observations but it cannot fully use the modern observation datasets and dynamical balances. With the rapid growth of modern observation systems, it is desirable to develop a method that can take advantage of both the modern statistical data assimilation techniques and the traditional objective analyses.

In this paper, we propose a sequential variational analysis approach that can effectively retrieve the resolvable information from observations at the initial steps of the sequence, after which the sequence of multiscale analyses smoothly evolves to a standard statistical variational analysis. The method introduced in this paper is named the Space and Time Multiscale Analysis System (STMAS) because it solves a sequence of variational problems from large to small scales and incorporates temporal information in the datasets, including in situ or remotely sensed data from radar, satellite, and microwave instruments. This sequential variational analysis can also employ proper balance and physical constraints at different analysis scales in the multiscale sequence; for example, geostrophic balance may be applied on the large scale, whereas appropriate balance relationships and numerical prediction models can be used as constraints at relatively small scales as in a 4DVAR scheme. We intend to fully use the spatial and temporal information from the observations, creating a flexible system for future extension to a sequential four-dimensional variational analysis using a numerical model as a constraint.

This approach was initially implemented for surface analysis using surface and temporal observation data but has been extended to a full three-dimensional spatial analysis system with a temporal analysis option. For the surface analysis applications, STMAS runs every 15 min on a 5-km grid in real time at the Global Systems Division (GSD) of the National Oceanic and Atmospheric Administration (NOAA) Earth System Research Laboratory (ESRL), with results available online (http://laps.noaa.gov/cgi/laps/domains/faa2km/ or http://laps.noaa.gov/request/nph-laps.cgi). STMAS is also being used at the Massachusetts Institute of Technology (MIT) Lincoln Laboratory (LL), where the STMAS surface analysis is being used as input to a boundary detection algorithm developed at LL for nowcasting in support of a Federal Aviation Administration (FAA) project to improve the automated Tactical Convection Weather Forecasts (TCWF; Wolfson et al. 2004).

This paper is organized as follows. In section 2, we review the techniques and difficulty in obtaining statistical error covariance and we compare a single 3DVAR and Barnes scheme using a response function analysis (a Fourier analysis). We then explain why a sequential variational analysis, such as STMAS, can result in much improved analyses. In section 3, we describe STMAS algorithms and implementation details. In section 4, we show some numerical comparisons of the analyses produced by the methods discussed here, a single 3DVAR, the Barnes scheme, and STMAS using an idealized, highly nonlinear, and multiscale test function. In section 5, we present numerical results using real datasets and verify the accuracy of our analysis. We also demonstrate the temporal impact of observations and dynamic constraints on the STMAS analysis. Concluding remarks are presented in section 6.

2. Comparing 3DVAR and successive corrections objective analyses

a. Error covariance in a standard variational analysis

The background and observation error covariance must be accurate in a three-dimensional variational analysis

based on the Bayesian theory (Lorenc 1986) to provide an accurate analysis within a certain probability. First, there is an assumption that these random errors of background and observations follow unbiased Gaussian distributions and the Gaussian covariance is accurate. Second, even if the covariance is accurate, an optimal analysis cannot be guaranteed, although it can be assumed to be the most probabilistically likely when the background and observation are treated as random vectors.

In general, it is very difficult to obtain an accurate background covariance. Many statistical approaches have been applied to obtain covariance estimations assuming the model background is an unbiased random vector representing the true atmosphere and include recursive filters (Hayden and Purser 1995; Purser et al. 2003a,b); the National Meteorological Center (NMC) method by Parrish and Derber (1992), the breeding vector method (Toth and Kalnay 1995; Pu et al. 1997), and ensemble approaches (Evensen 1994; Mitchell and Houtekamer 2000; Mitchell et al. 2002; Whitaker and Hamill 2002; Hamill et al. 2002). However, accurately estimating background error covariance for meteorological data assimilation remains a difficult statistical and computational problem. Even though the ''unbiased'' assumption is valid, the spatially and temporally dependent covariance requires a tremendous amount of case- and flow-dependent statistical samples since the number of control variables is usually $O(>1\ 000\ 000)$ for meteorological data assimilation. Generating these statistics is very expensive given the expense of running forecast models. Since the true atmosphere is unknown, forecast differences are usually used to estimate forecast errors under the unbiased assumption. These forecast differences can be computed by subtracting one forecast from another valid at the same time and they can be time-lagged, initial or boundary perturbed, or different model ensemble forecasts. The statistical correlations of these errors are used to estimate the error covariance. This approach can provide some information on the error covariance but it eliminates the diagnosis of major model bias even when a number of prediction models are used. The important model bias information will be missing in the estimated covariance.

An alternative approach for estimating the covariance would be to use the Kalman filter method. Running a Kalman filter in a long time sequence could provide not only a good error covariance but also a good analysis under the following assumptions: the forecast model is linear, observation simulation operators are linear, model and observation errors are unbiased, and the linear combination of the model and observation errors is the best error estimate of the true atmosphere. For nonlinear forecast models, a Kalman filter approach can be generalized but not theoretically proven to provide an accurate covariance in general applications. It is not difficult, however, to find studies where the Kalman approach fails in its covariance estimation (Julier and Uhlmann 1997). Thus, a classical Kalman filter is a good data assimilation technique for linear systems but may not be a good candidate for mesoscale meteorological data assimilation with respect to the high nonlinearity and high computational cost. To integrate forward in time, a full covariance matrix using the linear prediction model operator is extremely expensive for meteorological Kalman filter data assimilation.

The ensemble Kalman filter becomes an interesting tool for generating not only the forecasts but also the covariance (Evensen 1994; Julier and Uhlmann 1997; Mitchell and Houtekamer 2000, etc.). As an approximation to a classical Kalman filter method, EnKF inherits the above drawbacks of the classic Kalman filter. For large-scale meteorological features that are approximately linear, EnKF may effectively use a limited number of ensemble members to construct partial error covariance. When the covariance matrix is large, a small number of ensemble members are inadequate at specifying elements in the matrix. As Julier and Uhlmann (1997) discussed, at least $2N + 1$ members, where N is the number of controls, are needed to estimate the mean flow transported by a nonlinear system.

In summary, estimating the error covariance is a challenging and difficult problem. In fact, accurately estimating the covariance is essentially more difficult than solving the data assimilation problem itself. It is interesting that, to provide an analysis, one deals with N unknown states and grid values. But one faces an even more challenging problem in estimating $\frac{1}{2}N \times N$ unknowns for the symmetric covariance matrix using historical model forecasts.

However, as we have pointed out, more and more resolvable information is available in observational datasets. Each observation value contains information on all scales about the true atmosphere within the range of its observation error. All of these scales can be divided into two categories: (a) a part that can be resolved by given observation networks (i.e., relatively longer waves) and (b) a part that cannot be resolved by the networks but may possibly be estimated under a statistical analysis. We intend to propose a method that takes advantage of the resolvable and statistical information instead of applying a statistical analysis directly. For example, accurate frontal boundary information is usually missing from a model background field. If an observation network can observe the boundary, this is resolvable information that is retrievable. However, if the difference between the observations and model background were

treated as random errors, as is done in a standard 3DVAR, there would be little chance to define boundary structure correctly unless an accurate flow-dependent covariance was given. A two-step method would be more effective than a conventional statistical analysis. This proposed procedure would fully exploit the data to resolve real atmospheric features, followed by an application of statistical estimation for scales that cannot be resolved by the observation networks. For the second step of the statistical estimation, the error covariance of the method becomes a narrowly banded matrix and this statistical estimation is thus more efficient than the direct statistical approaches.

Before discussing this proposed method, let us review how an objective analysis retrieves resolvable information from observations. Even though many data assimilation techniques have been shown to be equivalent under the condition of a given accurate covariance (Lorenc 1986), a Barnes analysis (Koch et al. 1983; Hiemstra et al. 2006) is different in the sense that it does not require prior knowledge of the error covariance. The Barnes multiple-pass successive corrections scheme starts with an analysis for longer waves using a Gaussian function with a large influence radius. Its analysis scales are gradually reduced to smaller ones until the scales cannot be resolved by the observation networks. For in situ observations only and for a given error variance of an analyzed field, a single Barnes correction could result in a similar analysis to a 3DVAR. However, the Barnes scheme has difficulty handling remotely sensed datasets, such as radar radial winds and satellite radiances. Also, the traditional Barnes scheme cannot handle correlations between different analysis variables or physical balances and other constraints. A variational approach is more appropriate as it handles these requirements simultaneously in one minimization process.

b. Response analysis

In modern data assimilation, a 3DVAR has taken precedence over traditional successive corrections objective analyses such as the Barnes scheme because of the known limitations in handling advanced observations and physical constraints. However, discussion is rarely heard about 3DVAR limitations. In this study, we would like to explore the 3DVAR limitations when analyzing in situ observational data.

To demonstrate the difference between a Barnes analysis and a single 3DVAR for analyzing conventional data, a response function analysis for a single 3DVAR system using a recursive filter and a two-pass Barnes scheme is presented. The response function analysis helps us understand that STMAS (a sequential variational analysis approach) can be viewed as a variational extension of the Barnes scheme in space and time. Owing to the difficulty in obtaining an accurate error covariance, a simple recursive filter is widely used to approximate the covariance of a Gaussian error distribution for a model background field. This ensures the positive definiteness of the error covariance. Purser et al. (2003a,b) have introduced a more flexible anisotropic recursive filter but, as will be shown, the conclusions are not limited to our use here of simple recursive filters. The more general message of this discussion is that for any error covariance or filters used in 3DVAR, a successive correction analysis can be implemented using the same covariance information, and a single correction pass can yield the same analysis as 3DVAR. The simple recursive filter has the following form (see Hayden and Purser 1995):

$$u_i' = \alpha u_{i-1}' + (1-\alpha)u_i \quad \text{left pass},$$
$$u_i'' = \alpha u_{i+1}'' + (1-\alpha)u_i' \quad \text{right pass},$$

where u is a state variable of a 3DVAR analysis, u' is an intermediate filtered variable in one direction, and u'' is the filtered variable. The subscript index of i indicates the ith grid point of the dimension that the filter is applied. The α parameter is used to determine the filter's scale or the influence radius. A Fourier transformation of the recursive filter yields

$$(1-\alpha Z^{-1})\overline{u}' = (1-\alpha)\overline{u},$$
$$(1-\alpha Z)\overline{u}'' = (1-\alpha)\overline{u}', \tag{2}$$

or

$$\overline{u}'' = \frac{(1-\alpha)^2}{1-\alpha(Z^{-1}+Z)+\alpha^2}\overline{u} \tag{3}$$

for a single pass of a combination of the left- and right-pass filters, where $Z = e^{2i\pi/\lambda}$ is a unit complex number and λ is the horizontal wavelength; the bar over a variable stands for the Fourier transformation of that variable. This transformation shows how a recursive filter responds to different wavelengths of physical space. The transformed function is called its response function.

To compare this response function with that from the Barnes scheme, we first note that in a general form of the Barnes objective analysis (a successive correction scheme), a non-Gaussian error distribution function can also be used. Nonetheless, here a Gaussian is used to compare with the above 3DVAR using a recursive filter. Its $(k+1)^{\text{th}}$ iteration results in an analysis from its k^{th} iteration by the following equation:

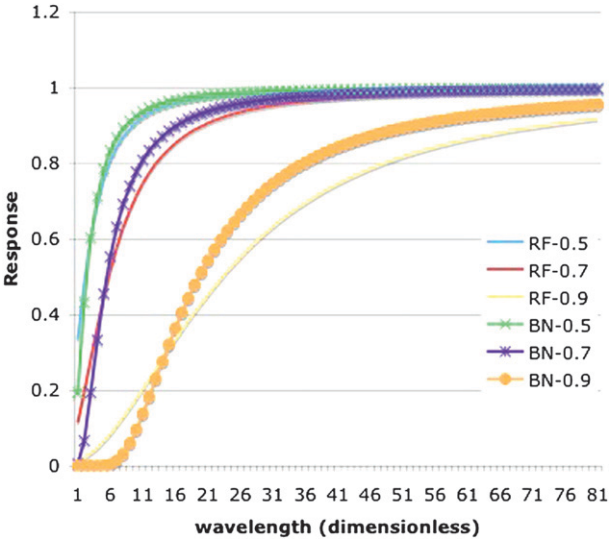

FIG. 1. Responses from a recursive filter (RF) and a Barnes iteration (BN). For example, RF-0.5 reflects the response of a recursive filter for $\alpha = 0.5$ while BN-0.5 represents a Barnes response from a parameter of $\kappa_0\gamma^k$ that makes its response closer to RF-0.5.

$$u_{k+1} = u_k + (o - u_k)e_k, \tag{4}$$

where

$$e_k = \exp\left(-\frac{d^2}{\kappa_0\gamma^k}\right) \tag{5}$$

and γ is the numerical convergence parameter that produces a scale reduction between two iterations, κ_0 is the initial iteration scale parameter, and d is the distance between the observation data o and a gridpoint location. The response function of this iteration has the following form (Koch et al. 1983):

$$\overline{e}_k = \exp\left[-\kappa_0\gamma^k\left(\frac{\pi}{\lambda}\right)^2\right]. \tag{6}$$

A simple comparison to relate these analyses is considered here. For the response function of a recursive filter with a given filter parameter α, we simply find a parameter $\kappa_0\gamma^k$ such that the response function of a single Barnes iteration is closest to the given recursive filter response function. Figure 1 shows the response functions of the recursive filter with $\alpha = 0.5$, 0.7, and 0.9 and the corresponding responses of a Barnes iteration, respectively, where the responses are plotted as functions of dimensionless wavelength $\lambda^* = \lambda/L$, where L is an arbitrary scale length. With a more careful selection of the parameters for the Barnes scheme, the Barnes response functions could be made to be even closer to the recursive filter curves.

We can see then that a 3DVAR analysis using a recursive filter is approximately equivalent to a single correction of the Barnes analysis using a Gaussian distribution. Hayden and Purser (1995) pointed out this equivalence when they studied the intrinsic scale of the recursive filter. In a more general sense, if the same error distribution function is used by a 3DVAR or a Barnes scheme, the 3DVAR is essentially equivalent to a single correction of the Barnes analysis. However, it is well known that an analysis from a single Barnes iteration does not yield a good objective analysis because multiple iterations are required. Since a single Barnes iteration cannot provide a good analysis, one cannot thus expect a good analysis from a 3DVAR either unless a good error covariance is available. This seems contradictory to the assumed optimality of a 3DVAR, but it is not if we are aware of the assumptions made. Let us review the necessary assumptions for this optimal 3DVAR.

In a 3DVAR derivation, observations and background errors are treated as random variables (Lorenc 1986) that statistically follow a certain Gaussian error distribution. If the Gaussian error covariance for background and observations are known, a 3DVAR is optimal with a known probability. Under the assumption that the error distribution is Gaussian and the covariance is known, the 3DVAR and the Barnes analysis with a single iteration are equivalent (Lorenc 1986). However, in practice, it is almost impossible to obtain a perfect or accurate error covariance. A Barnes analysis usually requires multiple iterations with different influence radii in the hopes of sweeping through all analysis scales and finding a better overall analysis by combining the analyses over these scales. However, this practice is far from optimal when the spatial distribution of the data is quite nonhomogeneous (Koch et al. 1983). Likewise, a single 3DVAR may not yield a good analysis if the covariance is unknown or contains incomplete or partial information. No strong evidence exists that shows that a 3DVAR analysis is in any way superior over a Barnes analysis with multiple iterations for conventional or in situ observation datasets. The advantages of using a 3DVAR over a Barnes analysis are in its ability to handle advanced observation data with specified error covariance, using covariance instead of variance, and imposing balance or constraints directly in the analysis instead of in a postprocessing stage. Hence, each of these two methods possesses their own respective superiority and limitations.

This response analysis could also provide a way to obtain a better variational analysis when there is useful resolvable information in the observations and background. We can apply a sequential variational method that mimics a Barnes scheme in a variational analysis context. A comparison of two response functions for

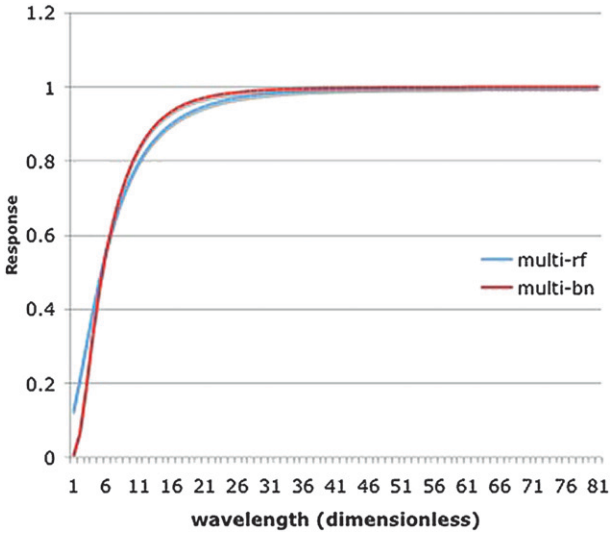

FIG. 2. Compositions of 2 response functions with RF-0.9 and RF-0.7 and with their counterparts by a Barnes scheme.

Barnes and 3DVAR using a recursive filter (Fig. 2) shows that a sequential variational approach can yield essentially the same response as a Barnes successive corrections scheme. For the resolvable scales in a given observation network, a sequential variational analysis can be made to match a Barnes analysis if the scheme can directly analyze the observation data. Thus, in a sequential variational approach, the resolvable information can be retrieved deterministically (i.e., no prior knowledge of the covariance) just like the Barnes scheme before becoming a statistical variational analysis. Furthermore, since a sequential variational analysis retains its variational attributes, it can handle all data sources, error covariances, and constraints appropriately. Thus, a sequential variational analysis possesses both advantages of variational and successive corrections analyses, and overcomes some of their individual limitations.

3. Space and Time Mesoscale Analysis System

A sequential variational analysis system called the Space and Time Multiscale Analysis System has been implemented at the NOAA Global Systems Division of the Earth Systems Research Laboratory. It utilizes spatial and temporal observations and is derived based on the response analysis described in the previous section. The basic idea is to iterate sequentially the variational analysis beginning at the larger scales and ending at the smallest resolvable ones (similar in that sense to successive correction approaches). Since a sequential variational analysis method can be implemented in many different ways as long as it can control the analysis scales at each of its iterations, we have developed and tested STMAS using a variety of procedures.

The first procedure tested is a straightforward implementation using a recursive filter. This version of STMAS starts with a variational analysis using a recursive filter with a large influence radius α in space and time (note the sizes of α are different in each dimension). After its initial variational solution, STMAS solves a similar variational analysis using a smaller influence radius α to resolve shorter waves contained in the residual between the previous analysis and the observations. This procedure may be repeated until no further analysis scales are resolvable by the observational data. Adding each sequence of analyses together produces the STMAS final analysis. This whole procedure is summarized as follows.

STMAS algorithm

Set large α's (e.g., 0.999)in each direction of space and time.

Step 1. Solve a variational minimization problem

$$\min(\mathbf{X}-\mathbf{X}^b)^{\mathrm{T}}\mathbf{B}^{-1}(\mathbf{X}-\mathbf{X}^b)+(\mathbf{HX}-\mathbf{Y}^o)^{\mathrm{T}}\mathbf{O}^{-1}\times(\mathbf{HX}-\mathbf{Y}^o)+\mathbf{P}, \quad (7)$$

where $\mathbf{X}^b$ is a background, $\mathbf{X}$ is the analysis at this variational sequence, $\mathbf{Y}^o$ is the observations, $\mathbf{H}$ is a mapping from grid space to observation locations, and $\mathbf{P}$ is a proper balance term added at this sequence of the analysis. The matrices of $\mathbf{B}$ and $\mathbf{O}$ are the error covariance for background and observation, respectively. For observation information retrieval, $\mathbf{B}$ can be set to $\beta(\mathbf{C}^{\mathrm{T}}\mathbf{C})^{-1}$ where $\mathbf{C}$ is the recursive filter operator and β is infinitely large unless a good estimation of $\mathbf{B}$ is available.

Step 2. Suppose the solution of step 1 to be $\mathbf{X}^a$. Set $\mathbf{X}^b=\mathbf{X}^a$ and $\mathbf{Y}^o=\mathbf{Y}^o-\mathbf{HX}^b$.

Step 3. Determine whether an additional analysis is needed (see the following discussion). If no further analysis sequence is needed, the final analysis will be the sum of the incremental analyses at all levels:

$$\mathbf{X}^{\text{final}}=\mathbf{X}_1+\mathbf{X}_2+\ldots\mathbf{X}_m$$

where $\mathbf{X}_j$ is the solution at the iteration sequence j. If further analysis is needed, go to step 4.

Step 4. Identify proper balance forming a penalty term as $\mathbf{P}$ and reduce α by $\tau\alpha$ where $\tau\in(0,1)$ and go to step 1.

Note that the background error covariance of the first term of (7) should change with different iterations to

obtain more scale-dependent information and further improve the analysis. However, in this paper, it is assumed to be constant; that is, it does not change with different scales. Future study will focus on this improvement.

One remaining question is how many of these iterations are necessary. STMAS employs the method of Koch et al. (1983) to determine how many iterations are needed to fully resolve the smallest scales that a given observational dataset can represent. Even though the recursive filters are isotropic, the final analysis increment of STMAS is fundamentally anisotropic because the increment is determined by the anisotropic difference between the background and observations. The recursive filter version of STMAS is implemented as follows: 1) an initial recursive filter parameter $\alpha = 0.999$ is used for the first variational analysis, and 2) this parameter α is then reduced by a fraction τ (=0.8) in each of the following 3DVAR solutions.

STMAS assimilates observations both spatially and temporally (i.e., the observations also have influence in temporal space over a certain length of time period). The recursive filter is applied not only in horizontal space but also in time space. Since STMAS was designed to provide a 5-km gridded analysis over the conterminous United States (CONUS) every 15 min (and 5 min in the future), we found that it is computationally too demanding to apply the recursive filter in all three dimensions (horizontal space and time) for this high-frequency product cycle. Moreover, parallelization of the recursive filter on multiprocessors presents additional complexity. It became necessary to test and compare more efficient implementations of STMAS. Hence, both a wavelet version of STMAS using cubic-spline base functions and a multigrid version were developed. Tests revealed that each version generated nearly identical analyses to the one produced using the recursive-filter version of STMAS (as discussed in section 4). This indicates that the particular numerical techniques have no bearing on the underlying science and performance. For a wavelet implementation, the STMAS algorithm remains the same except that $\mathbf{C} = \mathbf{I}$, an identity matrix, and $\mathbf{X}$ is replaced by a product of wavelet base functions and their correspondence coefficients. For a multigrid implementation, it is the same as the wavelet implementation except that $\mathbf{X}$ only has values at grid points for its multigrid levels. They are all variational, which minimizes the cost function of (7).

Because of its numerical efficiency and simplicity for parallelization compared to the recursive filter version of STMAS, a multigrid version STMAS was selected for operational surface analysis and boundary detection. As discussed above, each individual variational analysis requires a scale control mechanism. The multigrid implementation uses the number of grid points to control the analysis scales. For a given number of grid points over a given domain, only limited wave scales can be resolved. The more grid points there are, the smaller the scales that can be resolved. Therefore, a multigrid implementation of STMAS initially uses a coarse grid with fewer grid points in each spatial and temporal direction to limit short waves. This allows resolution of only the longest waves in its analysis. During each sequential pass, the number of grid points is doubled uniformly until the grid distance reaches a minimum, at which the observation networks provide no further resolvable information. Since the number of grid points controls the analysis scales, nothing further is required, although the technique can benefit whenever an appropriate error covariance can be estimated. Thus, each variational cost function of the sequence of analyses requires a simple interpolation from grid values to the values at observation locations for conventional data analysis, and a parallelization of this multigrid STMAS is straightforward.

The multigrid version of STMAS run for the surface analysis is so efficient that it only takes ~5 min to complete an analysis of eight variables with 5-km resolution over the Rapid Update Cycle (RUC) CONUS domain using a single processor with a clock speed of 3.2 GHz. A recursive filter version takes more than 30 min to complete the same analysis. To be precise, this CONUS domain has 1473×1025 horizontal grid points and employs 15-min time steps over a 90-min temporal window (thus, six time intervals of data are used). The reason for choosing a 90-min temporal window is based on the computation requirement for STMAS implemented using a recursive filter. It takes longer than our analysis cycle time to provide an analysis if a longer time window is used. Using a longer than 90-min time window for a multigrid version of STMAS does not result in a dramatic improvement.

Despite the tremendous number of surface observation sites available for the STMAS surface analysis, there are still large areas with relatively sparse observations interspersed with small regions of abundant observations, much like observation ''oases'' scattered with data ''deserts'' (Fig. 8). Neither successive correction (SC) schemes (such as the Barnes scheme) nor optimum interpolation (OI) nor 3DVAR analysis schemes adequately handle the desert–oasis (data nonhomogeneity) problem. For example, inhomogeneous station distributions cause problems for a fixed value of either the final-pass weighting function in successive correction methods or the covariance function scale in OI and 3DVAR methods. ''Overshooting'' is often seen in the data-sparse area as the schemes attempt to propagate information

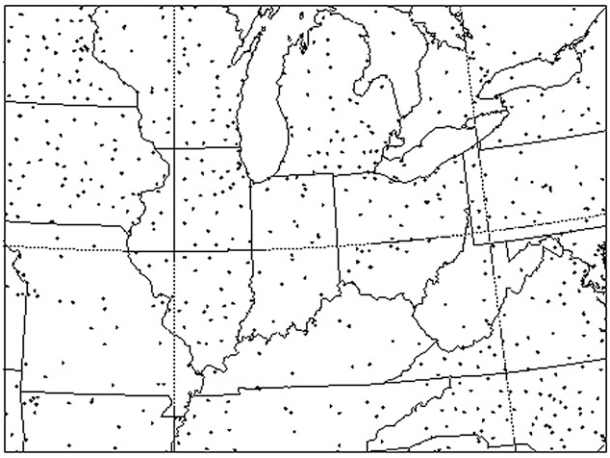

FIG. 3. MesoNet stations available in 2004.

from the oases to the deserts [see the discussion in Koch et al. (1983) about overshooting]. Typically, none of these schemes explicitly includes the high-resolution time information inherent in much of the mesonet data, with the single notable exception of a time-to-space conversion (TSC) extension of the Barnes scheme developed by Koch and O'Handley (1997) for the specific analysis of quasi-two-dimensional propagating features such as gravity waves. STMAS offers locally variant scales in its analysis and uses the temporal information (without the need to invoke the TSC approximation) to resolve the problem inherent between oases and deserts, particularly if some of the observations in sparse areas are intermittent.

4. Numerical experiments

In this section, an idealized experiment is presented to demonstrate the differences of the data assimilation methods discussed earlier. It is known that sharp frontal discontinuities, convective outflow boundaries, sea breeze convergence zones, and other mesoscale boundaries are usually missing from model backgrounds, or at least not accurately represented. If a relatively dense observation network (Fig. 3) can observe these boundaries, there is very useful information in the difference between background and observations. This provides the opportunity for an application of STMAS to diagnose the boundaries. These retrieved boundaries will have strong impact on short-range nowcasts and forecasts of deep convection, atmospheric dispersion, fire weather, and other applications. For this reason, in this idealized test case, a highly nonlinear, multiscale analytic function mimicking a complex bore/soliton phenomenon frequently associated with fronts or outflow boundaries (e.g., Koch et al. 2008) is constructed. Its two-dimensional

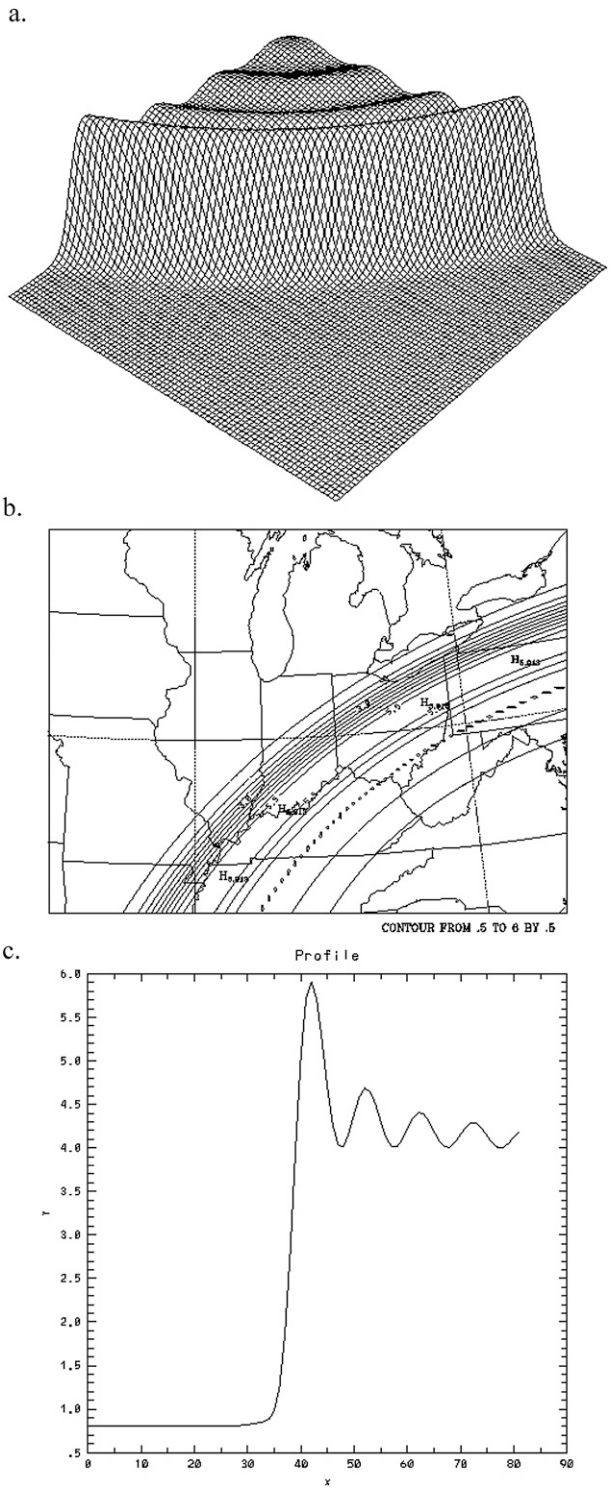

FIG. 4. The (a) 3D surface, (b) contour, and (c) profile plots of an analysis function.

horizontal contour plot, vertical profile, and a 3D visualization are shown in Fig. 4. We assume that this analytic function is a missing feature not resolved by a model background but is observed by a national mesonet network over the region shown in Fig. 3; (station locations are depicted as dots). In this experiment, we use the actual mesonet observation station locations available in 2004 and the analytic function values at these station locations as the observed values to test different data assimilation methods and see how they resolve the ''true'' feature.

We start with a 3DVAR method using a recursive filter on this idealized case. The main issue in using a 3DVAR with a recursive filter is the selection of the influence radius for the recursive filter (i.e., α for this simple recursive filter test), which is computed based on a statistical estimation in practice. As discussed earlier, determining the value of α is a difficult and poorly posed problem. Therefore, we examined several choices for α and discuss the results in analyzing the multiscale features of this test case. We selected $\alpha = 0.5$, 0.7, and 0.9 and ran a standard 3DVAR with each of these parameters, respectively. The results (Fig. 5) show that the analysis with $\alpha = 0.5$ produces an abundance of small-scale features. If this parameter value were applied in a real case where the true state of the atmosphere is not known, these small-scale features could be misinterpreted as mesoscale waves. Use of larger α values produces smoother analyses, but the small waves are lost relative to the dominant long wave because of the highly multiscale, nonlinear (non-Gaussian) character of the bore function. The multiscale character is a challenge for a data assimilation method like a single pass of a standard 3DVAR using a recursive filter.

To confirm our response analysis conclusions, we also applied a two-pass Barnes scheme over the ''observation data'' and obtained the analysis shown in Fig. 6. A single iteration of the Barnes analysis (not shown) gave results that are similar to those from the 3DVAR, but the two iterations of the Barnes scheme compare much better to the analytic function in Fig. 4 and approximate the front quite accurately. The positive aspect of this scheme results from it being a multiple iteration scheme that sweeps through finer-scale wavelengths. On the other hand, the amplitude-ordered wave train behind the bore front is poorly represented in the Barnes analysis (though it is decidedly better than in the 3DVAR). Thus, it is reasonable to expect a STMAS implementation to obtain a similar or better result.

We tested the recursive filter, wavelet, and multigrid versions of STMAS over the same datasets. Even though there are slight differences among these analyses (Fig. 7), they each captured the major wavelengths of the storm

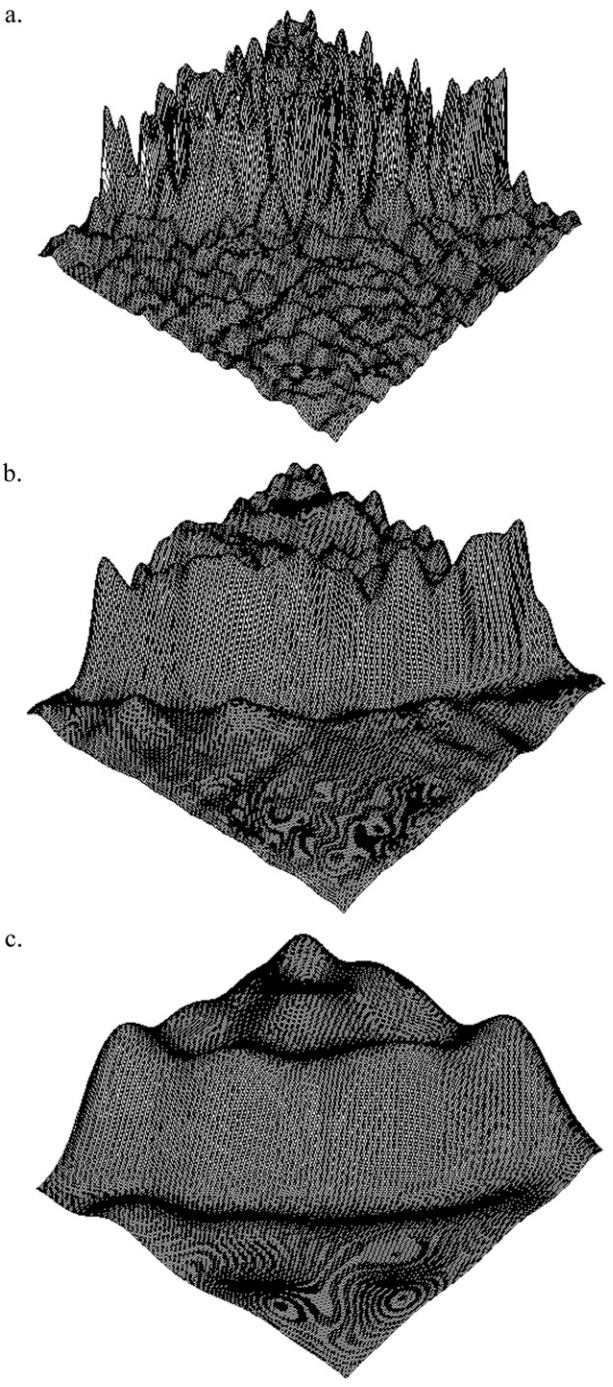

FIG. 5. Recursive filter 3DVAR analyses; α = (a) 0.5, (b) 0.7, and (c) 0.9.

boundaries from large to small better than either the 3DVAR or the Barnes scheme did. As we discussed in section 2, the analyses are anisotropic because of the multiple passes. Other arbitrary test functions were also tested, confirming that STMAS provides good analyses under a variety of scenarios. From this experiment, we

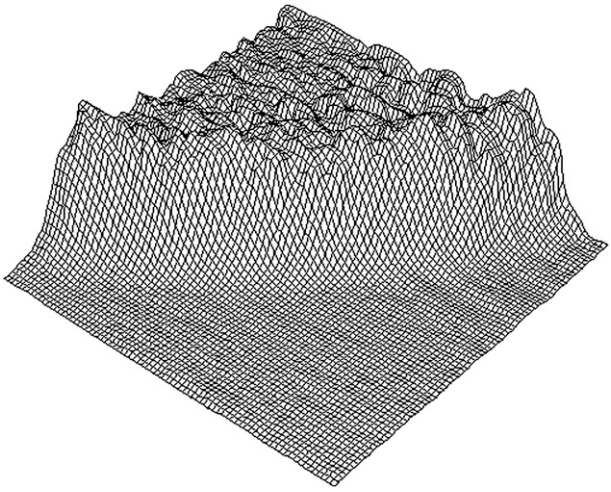

FIG. 6. A Barnes analysis with two iterations.

conclude that STMAS can handle multiscale analyses by using multiple iterations better than either a single 3DVAR or successive corrections approach. Its capability to handle remote sensing data from radar and satellite, as well as physical balances, will be investigated in future data assimilation.

From this analytic function experiment, we have demonstrated how well STMAS approximates an analytical front or boundary feature, consistent with the response function analysis. The following experiments illustrate STMAS' performance in an operational-like setting for automated storm boundary identification. These real data case studies serve as further verification of the STMAS analysis capabilities.

5. Numerical experiments on real surface mesonet data

a. Analysis accuracy verification

In this section, we further substantiate the accuracy of the STMAS analysis, demonstrate its inhomogeneous, multiscale analysis capability, and assess the temporal impact using actual mesonet data and the RUC 40-km model forecasts as background fields. The STMAS surface analysis utilizes all possible surface data sources through GSD's Meteorological Assimilation Data Ingest System (MADIS), including aviation routine weather reports (METARS), the coastal marine automated network (C-MAN), surface aviation observations (SAOs), the modernized cooperative observer program (COOP), and MesoWest. Table 1 lists the MesoNet providers available to MADIS in 2004, which at that time provided data from more than 13 000 stations. Today, more than

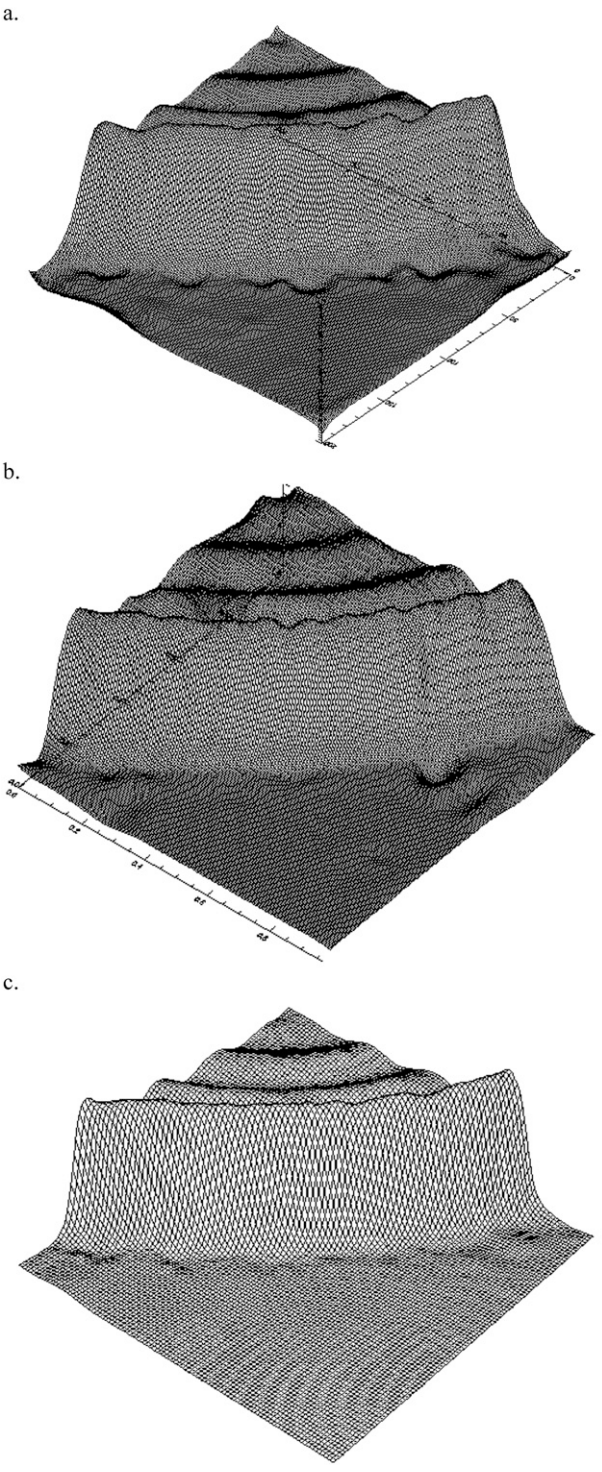

FIG. 7. STMAS analyses: (a) recursive filter, (b) wavelet, and (c) multigrid analyses.

50 000 stations are available over the United States (Fig. 8), and many of these stations are providing 1-min sampled data. STMAS is able to fully use these data made available through MADIS, a system that is becoming fully

TABLE 1. A list of MADIS MesoNet providers available on 11 May 2004.

MesoNet	Provider	No. of sites	Coverage
US. Army Aberdeen Proving Grounds	APG	5	Maryland
Citizen Weather Observer Program	APRSWXNET	2195	Global
AWS Convergence Technologies, Inc.	AWS	5600	U.S.
Anything Weather Network	AWX	64	CONUS
Colorado Department of Transportation	CODOT	107	Colorado
Florida MesoNet	FL-Meso	39	Florida
Ft. Collins Utilities	FTCOLLINS	5	Colorado
Goodland WFO Miscellaneous	GLDNWS	15	CO/KS/NE
Gulf of Maine Ocean Observing System	GoMOOS	10	Gulf of Maine
FSL ground-based GPS	GPSMET	340	U.S.
Hydrometeorological Automated Data System	HADS	60	New England
Iowa Department of Transportation	IADOT	50	Iowa
Iowa Environmental MesoNet	IEM	88	Iowa
Boulder WFO Miscellaneous	INTERNET	13	Colorado
Kansas Department of Transportation	KSDOT	41	Kansas
Multi-Agency Profiler Surface Observations	MAP	12	CONUS
Cooperative MesoNets in the western United States	MesoWest	2552	West CONUS
Minnesota Department of Transportation	MNDOT	92	Minnesota
National Ocean Service Physical Oceanographic Real-Time System	NOS-PORTS	34	CONUS
National Weather Service Cooperative Observer Program	NWS-COOP	100	New England
Oklahoma MesoNet	OK-Meso	116	Oklahoma
Remote Automated Weather Stations	RAWS	1777	U.S.
Radiometer	RDMTR	2	U.S.
Denver Urban Drainage and Flood Control District	UDFCD	17	Colorado
Weather for You	WXforYou	414	U.S.
		Total: 13 748	

operational in the National Weather Service. MADIS includes automated quality control, gross validity checks, temporal consistency checks, internal (physical) consistency checks, and spatial checks (see http://www-sdd.fsl.noaa.gov/MADIS), as well as a blacklist that can screen out stations with known issues.

STMAS is being used to provide surface mesoanalyses with temporal consistency for convective boundary identification, which is very important for some FAA applications (Wolfson et al. 2004). A real data case from 22 September 2005 is presented here as a demonstration of the marriage of the STMAS analysis with the Lagrangian Scalar Integration (LSI) method developed at MIT for the FAA (Jones and Winkler 2002). We also compare the objectively analyzed surface fronts against analyzed boundaries manually created at the Hydrometeorological Prediction Center (HPC; http://www.hpc.ncep.noaa.gov/sfc). The LSI technique can be applied to gridded surface analysis fields, which for this study is the STMAS analysis. LSI specifies a grid of tracers from a wind analysis at a resolution of interest and then advects the tracers following the horizontal winds. Data are gathered along each trajectory as a time series that is then time-averaged over some fixed integration period. At MIT LL, the LSI method is applied to the STMAS surface analysis over a region where the HPC boundary identification shows the location of the storm fronts. The automated analysis of fronts and other boundaries derived from this LSI time-integrated divergence technique is plotted in Fig. 9 and compared to the HPC analysis. The red and blue lines are the warm and cold fronts provided by the HPC analysis, and the underlying black and white images are the LSI-based products computed using STMAS. MIT and HPC produced these boundary detections independently. The detected boundaries are very close and they are almost identical at certain times. This indicates that the STMAS produced a meaningful analysis, allowing the automated boundary detection method to perform well; since STMAS uses temporal information, the gridded data reveal a smooth transition of the frontal boundaries. Together with the application of LSI, this enables the MIT detection algorithm to identify the boundaries accurately, which had not been possible based on other analyses.

In addition to the above qualitative verification, a quantitative comparison is presented here for STMAS and a standard 3DVAR using a recursive filter. Following traditional analysis evaluation metrics, we examined the root-mean-square (RMS) errors of the analyzed values compared to the observations over a region encompassing the eastern CONUS. Table 2 shows the RMS errors of the recursive filter version of the STMAS analysis

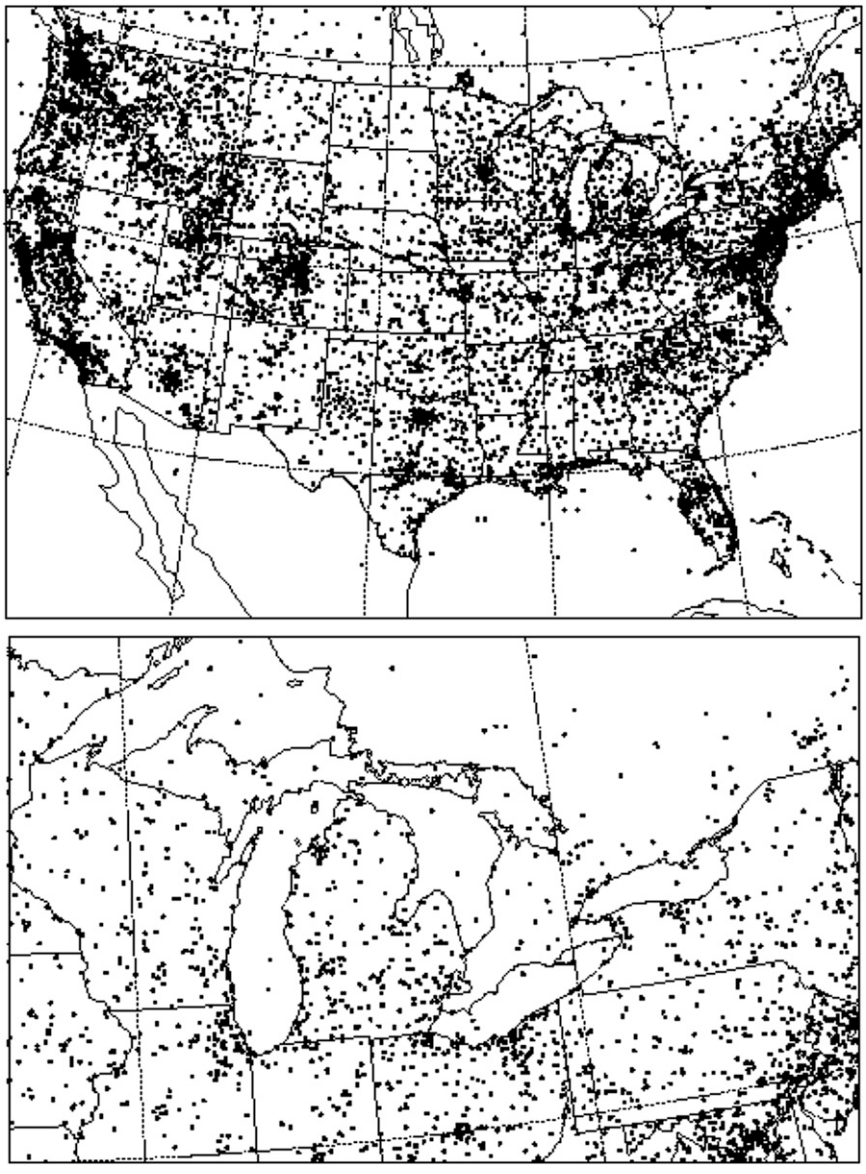

FIG. 8. National and regional maps of MesoNet stations available in 2008.

compared to those from a single 3DVAR with different α values over the same region. A smaller influence radius for the 3DVAR analysis has a negligibly smaller RMS error, which means it fits observations slightly better using smaller-scale waves than with larger-scale waves. By comparison, STMAS has decreased the RMS analysis error by roughly 50% relative to either 3DVAR analysis.

In the independent verifications against the HPC front analysis and through RMS errors, the STMAS surface analysis consistently shows accurate surface analyses with very fine detailed structure. The scheme is computationally very reliable and stable. The verification validates the conclusions we made in previous sections for Barnes, 3DVAR, and STMAS analyses.

b. *Temporal consistency*

An important feature of STMAS that could help ameliorate the effects of spatial and temporal inhomogeneity is its use of temporal information, since STMAS provides a temporally coherent analysis. For the operational STMAS analysis, a 90-min time window is set and the multigrid technique is also applied in this temporal domain. To illustrate the temporal impact on the analysis, we set two STMAS runs: one a 90-min time window,

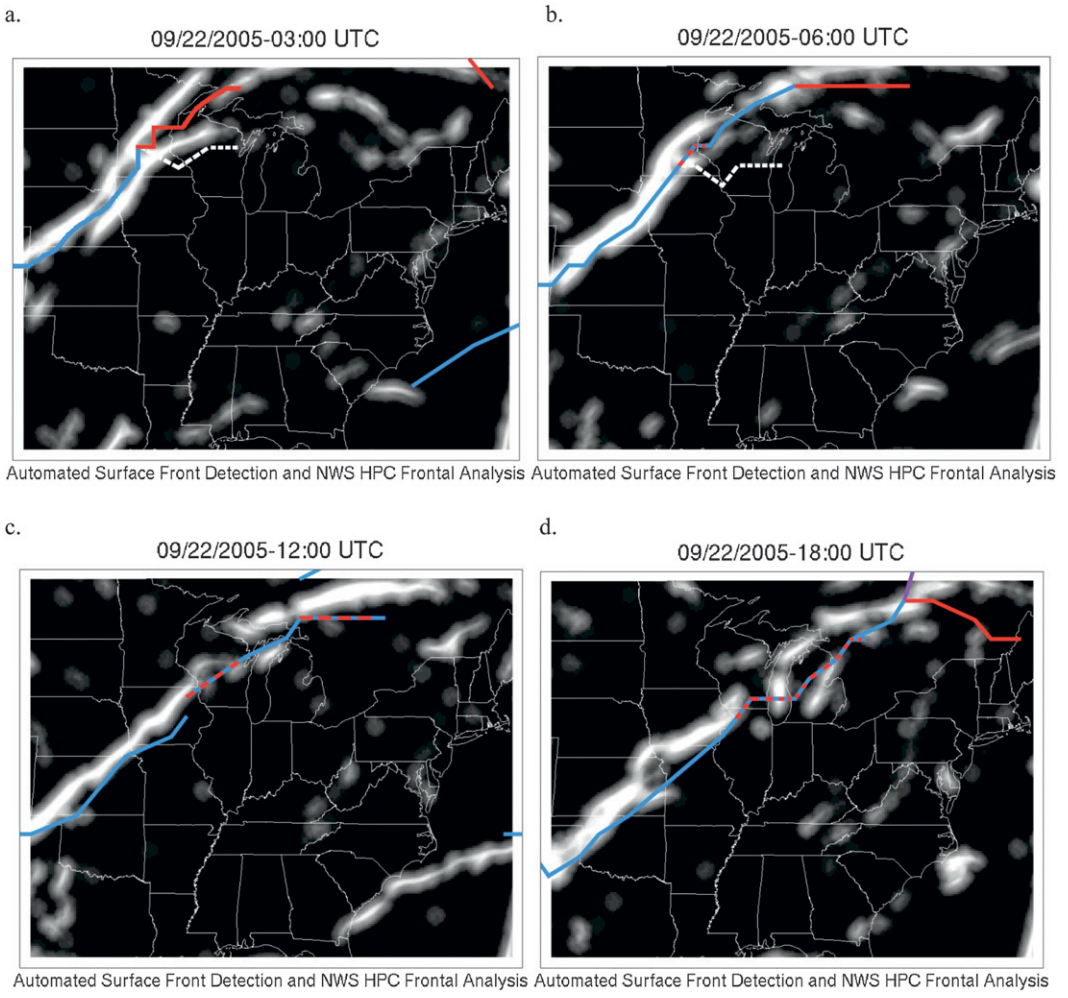

FIG. 9. Comparison between MIT LL and HPC boundary detections. Blue and red curves are the HPC boundary and the black and white images are the MIT–STMAS storm boundary. (a)–(d) The storm boundary propagation in 3-h intervals during 0300–1800 UTC 22 Sep 2005.

which is the standard STMAS configuration, and the other a 15-min time window. We compared their differences to assess the impact from assimilating temporal information. Figure 10 shows the 15-min dewpoint temperature analysis increments at 1600–1645 UTC 23 January 2008 on the left and the 90-min window analysis on the right. From 1600 to 1645 UTC, the 90-min dewpoint analysis smoothly changes and transitions through time, while the 15-min window analysis shows more discontinuity, particularly in the areas over Colorado, Kansas, Oklahoma, and Texas at 1615 UTC. The 90-min window analysis is likely a better depiction of the real atmosphere. This temporal impact is particularly helpful operationally since real-time observation datasets can vary rapidly in both coverage and quality for various reasons. For example, different report frequency, hardware failure, communication problems, and quality control, among others, all contribute to observational data variations in time. Table 3 lists the numbers of observation data that are actually ingested into the STMAS analysis every 15 min at 1600 UTC 23 January 2008. Even though the surface datasets are quite stable, they still vary from time to time by 10%. Regarding temporal continuity, by fully taking advantage of STMAS' computational efficiency, STMAS reduces the impact due to observation data temporal unavailability of observation data and temporal variability and provides more robust analyses. This advantage is extremely important for storm boundary detections.

TABLE 2. RMS errors (m s^{-1}) of the wind analysis against observations over an eastern CONUS domain.

Method	STMAS (recursive)	3DVAR ($\alpha = 0.5$)	3DVAR ($\alpha = 0.7$)
RMS errors	0.1173	0.2676	0.2831

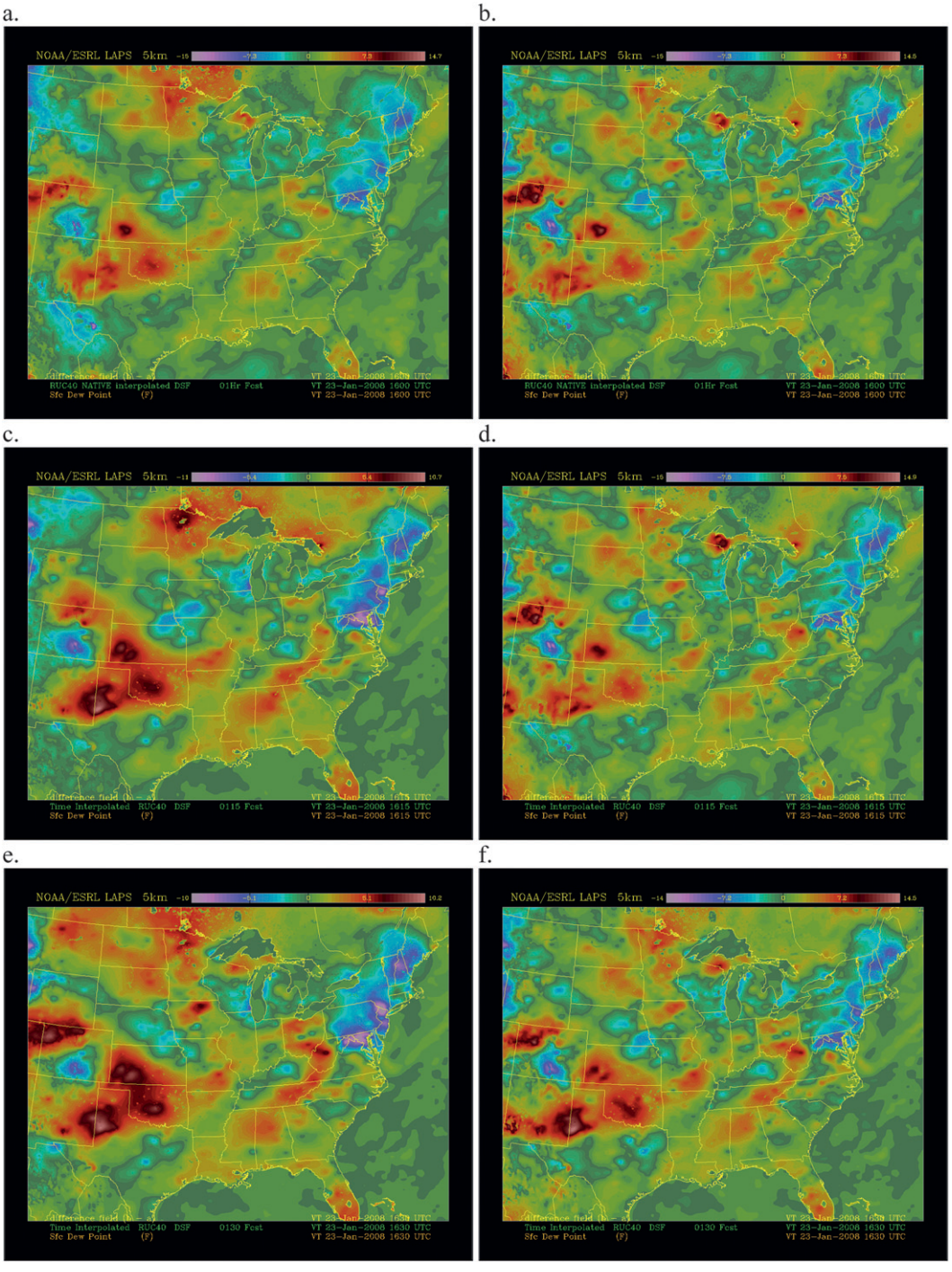

FIG. 10. STMAS dewpoint analysis with (left) 15-min and (right) 90-min temporal windows. The plots are at the exact same times even though the analyses use different temporal windows: (top to bottom) 1600, 1615, and 1630 UTC analyses.

c. *Full three-dimensional spatial analysis using STMAS*

From the above cases, STMAS is shown to improve 3DVAR analysis by handling multiple scales that are resolved by the observation network without using any statistical information. It saves the statistical computation for finer-scale data assimilation that will be demonstrated in the near future. The combination of a modern variational analysis and a traditional objective analysis

TABLE 3. Number of observations at every 15-min temporal window.

Time window (UTC)	No. of valid dewpoint observations
1600–1615	8499
1615–1630	8879
1630–1645	8022
1645–1700	7790
1700–1715	8705

has not demonstrated how STMAS handles balances and remotely sensed data in the above STMAS surface analysis. To show STMAS reduces a traditional objective analysis limitation on handling balance and modern observation datasets, we consider a full four-dimensional analysis over a pressure coordinate, where geostrophic and/or hydrostatic balances can be applied.

A fully four-dimensional (3D spatial plus temporal) version of STMAS has also been applied to several severe weather situations. These results will be fully presented in a separate paper. However, initial results for various three-dimensional applications of STMAS are very encouraging. Some initial forecast impacts show that with the geostrophic and hydrostatic balances, STMAS reduces the initial shock waves when it initializes an Advanced Research Weather Research and Forecasting model (ARW–WRF) forecast. For the Hurricane Katrina test case, at the initial hours (3 and 6 h) of WRF forecasts, the STMAS analysis with these balances only increases the central pressure by 2–3 millibars, as compared to 20 millibars if a Barnes scheme is used. STMAS indeed improves a Barnes analysis by directly applying dynamic balances as constraints in its minimization of the cost function. An analysis of Hurricane Dennis on 11 July 2005 was performed using both conventional in situ and a gridded airborne radar dataset. STMAS-3D analyzed these datasets remarkably well and captured the detailed hurricane structure. The u and v components of the wind at 850 hPa are shown in Fig. 11. The STMAS multiscale analysis capability can be seen clearly in the increment field; for example, the u-component increment in Fig. 12 shows finer-scale features over the area covered by airborne radar data and relatively large-scale features elsewhere.

In summary, the STMAS idealized and surface cases show how STMAS improves modern variational analysis and the later full four-dimensional case demonstrates how STMAS improves a traditional objective analysis by using modern observation datasets and applying dynamical balances. STMAS indeed combines the advantages of both variational and objective analyses and reduces their limitations respectively.

6. Conclusions

A sequential, multiscale variational analysis scheme—the Space and Time Multiscale Analysis System (STMAS)—has been developed. STMAS possesses the advantages of both a traditional successive corrections technique and modern variational analysis while addressing their limitations. Examination of the response functions for each scheme provided a basic understanding of the difference between a 3DVAR and a traditional

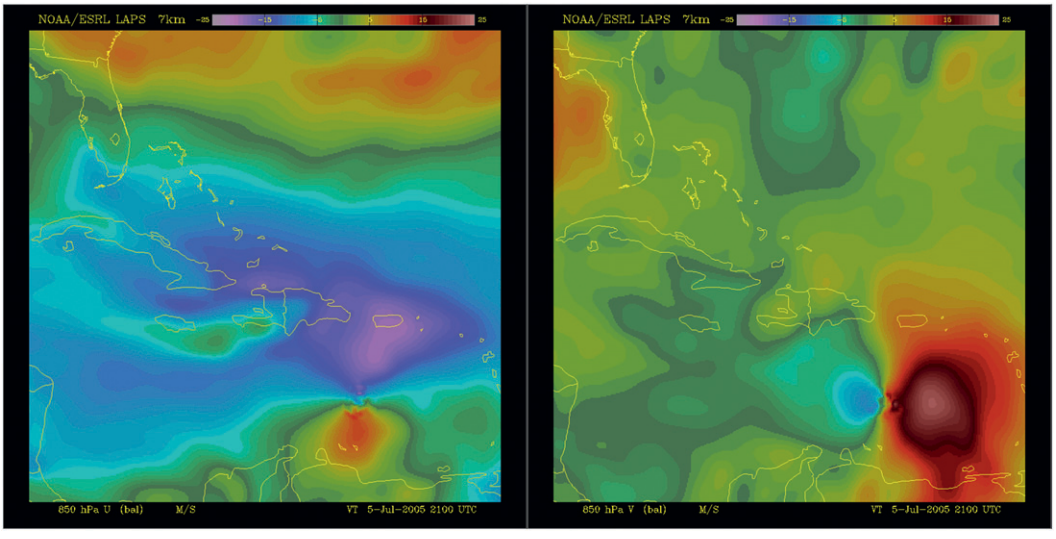

FIG. 11. STMAS 3D analysis of Hurricane Dennis at 850 hPa at 2100 UTC 5 Jul 2005: (left) u component; (right) v component. The color bar shows 10-m s^{-1} intervals from −25 to 25 m s^{-1}.

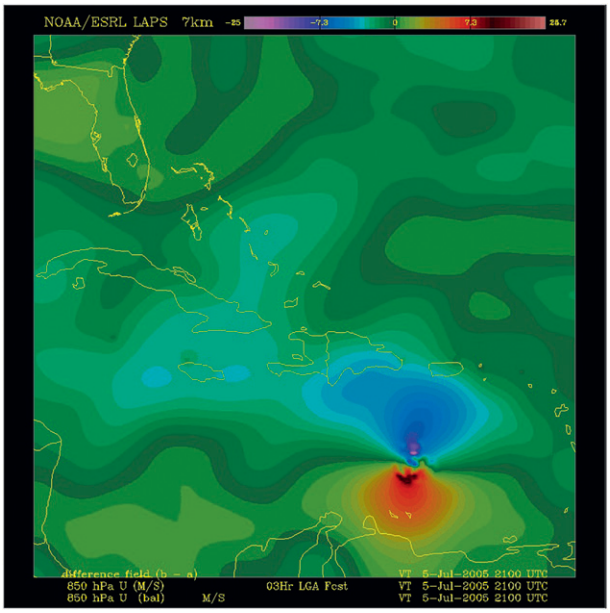

FIG. 12. The *u*-increment field of the STMAS 3D analysis of Hurricane Dennis at 850 hPa.

Barnes analysis. Additional insight about the differences in their behavior was gained from an idealized analytic function designed to mimic a highly nonlinear, multiscale phenomenon. STMAS greatly outperformed both of the other approaches in that idealized experiment. We demonstrated STMAS' capability to produce a multiscale analysis while also showing that a standard 3DVAR has difficulty in managing all of the resolvable scales when an accurate covariance is unavailable. STMAS was then tested using a recursive filter, wavelet approach, and a multigrid method, and the multigrid version was then chosen for real-data applications.

In subsequent real-data experiments, we demonstrated the value of using the STMAS analysis in combination with a Lagrangian scalar integration method to objectively detect storm boundaries. A comparison of the results to the HPC boundary analysis verified the quality of the STMAS–Lagrangian analysis method. We also compared the analysis error from STMAS to that from a standard 3DVAR using a recursive filter for estimating the covariance. This comparison demonstrated the substantial positive impact provided by the temporal consistency in STMAS. We further confirmed that STMAS indeed provides accurate multiscale, inhomogeneous, and temporally consistent analyses using model background and observations.

STMAS shows potential to be a full three-dimensional spatial analysis scheme, including the ability to handle remotely sensed datasets. This full analysis holds promise for providing accurate nowcasts and for initializing numerical prediction models. In the near future, STMAS' full three-dimensional spatial analysis could take advantages of its 3D variational attributes for handling radar, satellite, physical constraints, and error covariance, though it is likely that the code will need to be parallelized as the computation becomes more intense. The multigrid STMAS will greatly reduce the complexity of parallelization compared to its recursive filter version counterpart.

More future work is needed for improving STMAS analysis for nowcasting and forecasts. In this paper, STMAS assumes the background and observation error covariance are invariant from coarse grid to fine grid. More sophisticated and scale-dependent error covariance would further improve STMAS analysis. This will be studied in the near future.

Acknowledgments. The authors thank Dr. Ning Wang of Global Systems Division, Earth System Research Laboratory of NOAA for implementing a wavelet version of STMAS and providing its results from an analytical test case. We also appreciate the editing effort by Ms. Ann Reiser and Dr. Seth Gutman of GSD.

This research is in response to requirements and funding by the Federal Aviation Administration (FAA). The views expressed are those of the authors and do not necessarily represent the official policy or position of the FAA.

REFERENCES

Bouttier, F., and P. Courtier, cited 1999: Data assimilation concepts and methods. F. Bouttier and P. Courtier, Eds., ECMWF. [Available online at http://www.ecmwf.int/newsevents/training/rcourse_notes/DATA_ASSIMILATION/ASSIM_CONCEPTS/Assim_concepts.html.]

Courtier, P., and O. Talagrand, 1987: Variational assimilation of meteorological observations with the adjoint vorticity equation. Part II. Numerical results. *Quart. J. Roy. Meteor. Soc.,* **113,** 1329–1347.

Evensen, G., 1994: Sequential data assimilation with a nonlinear quasi-geostrophic model using Monte Carlo methods to forecast error statistics. *J. Geophys. Res.,* **99** (C5), 10 143–10 162.

Hamill, T. M., C. Snyder, and R. E. Morss, 2002: Analysis-error statistics of a quasigeostrophic model using three-dimensional variational assimilation. *Mon. Wea. Rev.,* **130,** 2777–2790.

Hayden, C. M., and R. J. Purser, 1995: Recursive filter objective analysis of meteorological fields: Applications to NESDIS operational processing. *J. Appl. Meteor.,* **34,** 3–15.

Hiemstra, C. A., G. E. Liston, R. A. Pielke Sr., D. L. Birkenheuer, and S. C. Albers, 2006: Comparing Local Analysis and Prediction System (LAPS) assimilations with independent observations. *Wea. Forecasting,* **21,** 1024–1040.

Jones, C., and S. Winkler, 2002: Invariant manifolds and Lagrangian dynamics in ocean and atmosphere. *Handbook of Dynamical Systems,* Vol. 2, B. Fiedler, Ed., Elsevier, 55–92.

Julier, S. J., and J. K. Uhlmann, 1997: New extension of the Kalman filter to nonlinear systems. *Signal Processing, Sensor Fusion,*

and Target Recognition, I. Kadar, Ed., International Society for Optical Engineering (SPIE Proceedings, Vol. 3068), 182–193.

Koch, S. E., and C. O'Handley, 1997: Operational forecasting and detection of mesoscale gravity waves. *Wea. Forecasting,* **12,** 253–281.

——, M. desJardins, and P. J. Kocin, 1983: An interactive Barnes objective map analysis scheme for use with satellite and conventional data. *J. Climate Appl. Meteor.,* **22,** 1487–1503.

——, C. Flamant, J. W. Wilson, B. M. Gentry, and B. D. Jamison, 2008: An atmospheric soliton observed with Doppler radar, differential absorption lidar, and molecular Doppler lidar. *J. Atmos. Oceanic Technol.,* **25,** 1267–1287.

Lewis, J. M., and J. C. Derber, 1985: The use of adjoint equations to solve a variational adjustment problem with advective constraints. *Tellus,* **37A,** 309–322.

Lorenc, A. C., 1981: A global three-dimensional multivariate statistical interpolation scheme. *Mon. Wea. Rev.,* **109,** 701–721.

——, 1986: Analysis methods for numerical weather prediction. *Quart. J. Roy. Meteor. Soc.,* **112,** 1177–1194.

Mitchell, H. L., and P. L. Houtekamer, 2000: An adaptive ensemble Kalman filter. *Mon. Wea. Rev.,* **128,** 416–433.

——, ——, and G. Pellerin, 2002: Ensemble size, balance, and model-error representation in an ensemble Kalman filter. *Mon. Wea. Rev.,* **130,** 2791–2808.

Parrish, D. F., and J. C. Derber, 1992: The National Meteorological Center's spectral statistical-interpolation analysis system. *Mon. Wea. Rev.,* **120,** 1747–1763.

Pu, Z.-X., E. Kalnay, D. Parrish, W. Wu, and Z. Toth, 1997: The use of bred vectors in the NCEP global 3D variational analysis system. *Wea. Forecasting,* **12,** 689–695.

Purser, R. J., W.-S. Wu, D. F. Parrish, and N. M. Roberts, 2003a: Numerical aspects of the application of recursive filters to variational statistical analysis. Part I: Spatially homogeneous and isotropic Gaussian covariances. *Mon. Wea. Rev.,* **131,** 1524–1535.

——, ——, ——, and ——, 2003b: Numerical aspects of the application of recursive filters to variational statistical analysis. Part II: Spatially inhomogeneous and anisotropic general covariances. *Mon. Wea. Rev.,* **131,** 1536–1548.

Toth, Z., and E. Kalnay, 1995: Ensemble forecasting at NCEP and the breeding method. NCEP Office Note 407, 55 pp.

Whitaker, J. S., and T. M. Hamill, 2002: Ensemble data assimilation without perturbed observations. *Mon. Wea. Rev.,* **130,** 1913–1924.

Wolfson, M. M., and Coauthors, 2004: Tactical 0-2 hour convective weather forecasts for FAA. *Extended Abstracts, 11th Conf. on Aviation, Range, and Aerospace Meteorology,* Hyannis, MA, Amer. Meteor. Soc., 3.1. [Available online at http://ams.confex.com/ams/11aram22sls/techprogram/paper_81242.htm.]